An investigation of space weathering on the Moon with mineralogy and hydroxyl. T. W. Hayes[1,2], C. A. Nixon[2], C. L. Young[3], M. S. Grant[3], S. Li[4], T. D. Glotch[5]. [1]Southeastern Universities Research Association, [2]NASA Goddard Space Flight Center, [3]NASA Langley Research Center, [4]University of Hawai'i – Manoa, [5]Stony Brook University.

Introduction: The possibility of the presence of water (hydrogen-bearing substances such as H_2O and OH) on the Moon was first brought about by samples returned by the Apollo missions. Since then, numerous additional evidence, such as detections of adsorbed hydroxyl (OH) and anomalous polar neutron flux, further support this concept [1-4]; and recently, the presence of molecular water on the Moon has been confirmed at the local scale [5]. Water is not just a crucial ingredient for life, in general; in the lunar context, it is an analog to the behavior of volatiles on other airless bodies and is a potential resource for future exploration missions. Previous studies suggest that the lunar regolith alone may host a significant reservoir of water [6] and underline the importance of locating regions of interest for extraction or future analyses. To pursue this goal, however, the origin and evolution of water on the Moon must be better constrained and understood.

One potential explanation for the origin and upkeep of water in the lunar environment is through the collection of processes called space weathering. Surfaces exposed to these processes generally alter over time and experience shifts in optical properties and chemical and physical changes [7]. Sources of water can be attributed to space weathering, whether via asteroidal or cometary impact [8] or through solar wind implantation [9]. The latter has been proposed to be capable of inducing a lunar water cycle when combined with other surface processes such as ballistic ejection and rehydroxylation [9]. This study seeks to investigate the possible link between regolith alteration and water production as evidenced by lunar spectra from the Diviner Lunar Radiometer and Moon Mineralogy Mapper (M3). To deduce the degree of space weathering, the optical maturity parameter OMAT defined by [10] will be used.

Multi-instrument data: The Diviner Lunar Radiometer instrument has three channels designed specifically to measure the Christiansen Feature (CF) of the Moon, globally. This feature corresponds to silica abundance, with shorter and longer wavelengths indicating silica-rich and silica-deficient compounds, respectively. Diviner CF values have been used to map global silicate mineralogy previously, as well as have been shown to be influenced by space weathering. Lucey et al. (2017) [11] showed that the slight shifts in CFs that result from space weathering can be partly mitigated by accounting for overall surficial maturity. Removal of these shifts are necessary to increase accuracy of CF value interpretations; however, these data cannot be completely disregarded. These shifts enable the quantification of the degree of space weathering experienced by a surface and can therefore be used as additional information to investigate and classify its impact on the lunar regolith and to OH therein.

Moon Mineralogy Mapper observations provide measurements on lunar OH levels, which have been have used to produce a global OH abundance map [6]. However, M3 OH data is not unique to one form of water; derived OH abundances can be indicative of actual OH, H_2O, or of OH-bearing minerals like apatite. Their OH map employs a thermal correction method derived from Diviner data as described in [12].

Data for Diviner CF values has been obtained from available global data products on the Planetary Data System and independently calculated. OMAT values have been retrieved from the USGS. M3-derived OH abundances are provided by [6].

Methods: In order to search for potential links between these datasets by investigating subtle shifts in CF maxima and their correlations to OH abundance and OMAT, we employ machine learning and statistical analyses such as a Bayesian classifier. Unsupervised machine learning methods such as Hierarchical or K-means Cluster Analysis (HCA and KCA) limit outside biases and result in natural groupings of data; moreover, they have proven useful for distinguishing spectra and spectral properties in previous studies on other airless bodies. We will firstly apply these techniques to CF values, CF value shifts from OMAT values, and OH abundances independently, then to a combined dataset so as to discern the reason for the formation of each cluster. Our Bayesian classifier uses prior probabilities based on native data distributions.

Our independently calculated CF data are binned into 4 pixels per degree (ppd) and reflects previously-reported CF values between the latitudes of 75ºN / 75ºS; data falling outside that region are not considered. Corresponding to nominal CF values reported in literature, we further remove all values less than 7.6 μm and greater than 8.6 μm, which almost entirely includes data only from our noisy polar sections. Results from [6] report accuracy for OH abundance between 85ºN / 85ºS, which will be restricted to match the spatial level of our CF data, as well as resampled to match the 4 and 32 ppd CF maps. OMAT values will also be resampled to match these spatial resolution levels.

Preliminary Results and Future Work: Our current results using HCA on lunar CF and OH abundance values show that machine learning is capable of distinguishing lunar petrology and overall water abundance. Maria, highlands, and several transition zones result in clusters and additionally follow large craters in our low resolution dataset. HCA on OH abundance mimics the poleward gradient seen in [6].

Using the distributions that naturally occur within CF and OH datasets, we have developed a Bayesian classifier that maps the surface into four classes. Prior probabilities for this classifier were determined from the main modes of data, highlighting highlands and maria for CFs (centered at 8.16 μm and 8.30 μm, resp.) and regions of low and high OH abundance (20ppm and 100ppm). The order of most to least likely classification is low OH highland, high OH highland, low OH maria, high OH maria, which is a fairly obvious trend given the comparison of area size of maria to highland and that OH increases primarily latitudinally. The distribution for these classes in the CF vs. OH space are shown in figure 1, and their application to the lunar surface is shown in figure 2. In the future we look to further parse these classes by mineralogy and region. Initial attempts highlight crater rims (e.g. Plato, Posidonius, and le Monnier), and portions of northern hemisphere maria and mountains. Pyroclastic deposits, dark, low albedo regions visibly similar to maria, are currently being grouped into the 'High OH Maria' class. This grouping is likely a result of some pyroclastic deposits having increased FeO abundances [13], which the CF is also related to, but will need further investigation to make a distinction between these regions. This classifier currently uses uncorrected CF values and therefore retains information for the degree of space weathering. We are eager to compare these results with corrected CF values. Our Bayes classifier will additionally lay the ground work for future applications of neural networks, as it enables us to develop a labeled training set of lunar data. As this classifier advances, it may also prove helpful in locating previously undiscovered pyroclastic deposits.

References: [1] Clark, R. N. (2009) *Science* 326, 562-564. [2] Sunshine, J. M., et al. (2009) *Science* 326, 565-568. [3] Pieters, C. M., et al (2009) *Science* 326, 568-572. [4] Sanin, A., et al. (2016) *EGUGA* EPSC2016-7169. [5] Honniball, C. I., et al. (2020) *Nature Astronomy* 1-7. [6] Li, S., et al. (2017) *Science Advances* 3(9), e1701471. [7] Hapke, B. (2001) *JGR Planets* 106, 10039-10073. [8] Svetsov, V. V., et al. (2015) *Planetary and Space Sciences* 117, 444-452. [9] Jones, B. M., et al. (2018). *GRL* 45(20), 10-959. [10] Lucey, P. G., et al. (2000) *JGR Planets* 105(E8), 20377-20386. [11] Lucey, P. G., et al. (2017) *Icarus* 283, 343-351. [12] Li, S., et al. (2016) *JGR Planets* 121(10), 2081-2107. [13] Allen C. C., et al. (2012) *JGR Planets* 117, E12.

Figure 1: CF-OH class counts from bimodal distributions and prior probabilities

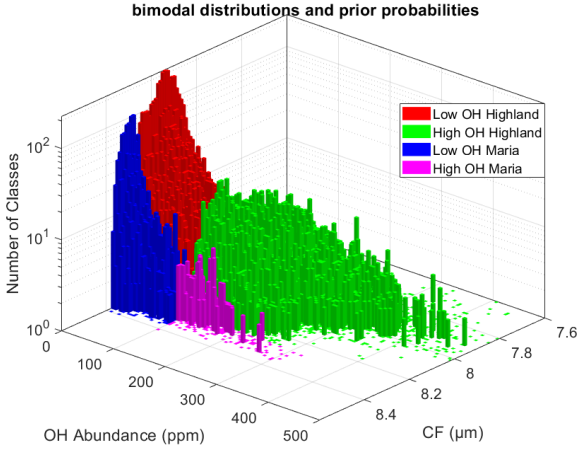

Figure 1: The distribution of CF and OH abundance data, color coded to highlight the four modal classes.

Figure 2: Four Bayesian classes applied to the lunar surface. Final classes were determined by the highest posterior probability for each location. Class coverage percentages are as follows:
Low OH Highland – 52.37%
High OH Highland – 37.15%
Low OH Maria – 9.48%
High OH Maria – 1.00%

Figure 2: Bayesian classes applied to the lunar surface